

Solution properties of γ -crystallins: Compact structure and low frictional ratio are conserved properties of diverse γ -crystallins

Yingwei Chen,¹ Huaying Zhao,² Peter Schuck,² and Graeme Wistow^{1*}

¹Section on Molecular Structure and Functional Genomics, National Eye Institute, National Institutes of Health, Bethesda, Maryland 20892-0608

²National Institute of Biomedical Imaging and Bioengineering, National Institutes of Health, Bethesda, Maryland 20892-0608

Received 12 August 2013; Revised 29 October 2013; Accepted 31 October 2013

DOI: 10.1002/pro.2395

Published online 9 November 2013 proteinscience.org

Abstract: γ -crystallins are highly specialized proteins of the vertebrate eye lens where they survive without turnover under high molecular crowding while maintaining transparency. They share a tightly folded structural template but there are striking differences among species. Their amino acid compositions are unusual. Even in mammals, γ -crystallins have high contents of sulfur-containing methionine and cysteine, but this reaches extremes in fish γ M-crystallins with up to 15% Met. In addition, fish γ M-crystallins do not conserve the paired tryptophan residues found in each domain in mammalian γ -crystallins and in the related β -crystallins. To gain insight into important, evolutionarily conserved properties and functionality of γ -crystallins, zebrafish (*Danio rerio*) γ M2b and γ M7 were compared with mouse γ S and human γ D. For all four proteins, far UV CD spectra showed the expected β -sheet secondary structure. Like the mammalian proteins, γ M7 was highly soluble but γ M2b was much less so. The heat and denaturant stability of both fish proteins was lower than either mammalian protein. The ability of full-length and truncated versions of human α B-crystallin to retard aggregation of the heat denatured proteins also showed differences. However, when solution behavior was investigated by sedimentation velocity experiments, the diverse γ -crystallins showed remarkably similar hydrodynamic properties with low frictional ratios and partial specific volumes. The solution behavior of γ -crystallins, with highly compact structures suited for the densely packed environment of the lens, seems to be highly conserved and appears largely independent of amino acid composition.

Keywords: crystallin; protein evolution; protein stability; solution behavior

Introduction

The vertebrate lens is subject to strong selective pressures because of species habitat and require-

ments for vision. The consequent adaptation of the lens in different lineages has led to variability in its protein composition, principally in the highly abundant, soluble crystallins.¹ In fish and in mammals, the major lens proteins are the α -, β -, and γ -crystallins.^{2,3} In particular, γ -crystallins predominate in the high refractive index lenses of fish and rodents and in the central lens nucleus of many species. These proteins, which are also evolutionarily related to β -crystallins, share a common, symmetrical, two-domain architecture.⁴ Each domain is formed from a

Grant sponsor: Intramural Research Programs of the National Eye Institute and the National Institute of Biomedical Imaging and Bioengineering at the National Institutes of Health.

*Correspondence to: Graeme Wistow; Section on Molecular Structure and Functional Genomics, National Eye Institute, Bg 6, Rm 106, National Institutes of Health, Bethesda, MD 20892-0608. E-mail: graeme@helix.nih.gov

pair of highly similar, modified “Greek key” motifs, each containing an unusual folded β -hairpin, intercalated to form a sandwich of two antiparallel β -sheets with a tyrosine corner.⁵ In mammalian γ -crystallins, each domain also contains a pair of conserved Trp residues, which contribute to the packing of the hydrophobic core of each domain and also exhibit strong quenching of UV fluorescence.^{6,7}

The protein surface of mammalian γ -crystallins is also notable for extensive networks of interacting polar side chains that may contribute to stability of folded structure while reducing the volume of bound water.⁸ The amino acid composition of mammalian γ -crystallins is also unusual, with relatively high contents of sulfur-containing residues, cysteine, and methionine. This has long been regarded as a potential liability and oxidation of cysteine and methionine has been linked to age-related cataract in humans.^{9–11}

In fish, the major γ -crystallins belong to the phylogenetically distinct γ M-crystallin class,^{12,13} which makes up about 30% of the lens protein in zebrafish (*Danio rerio*).¹⁴ These proteins have an even higher content of methionine (up to 15%) than mammalian γ -crystallins. Recently, a compelling explanation for the unusual amino acid composition of γ -crystallins (which also includes high levels of other large side chains such as aromatics and arginine) has been proposed.^{15–17} Individual amino acids make their own contributions to protein refractive index increments. The composition of crystallins, particularly of γ -crystallins, gives them significantly higher molecular refractive index increments than most other proteins. Thus, amino acid composition may have been selected for in the evolution of crystallins, particularly in the high refractive index (RI) fish lens. All vertebrate lenses maintain a gradient of RI from the outer layers of fiber cells to the dense core or nucleus. For the relatively soft human lens, the RI of the nucleus has been measured at 1.42 by optical coherence tomography,¹⁸ while for adult zebrafish the equivalent value was 1.54,¹⁹ For a range of vertebrates, the RI gradient has been measured by x-ray Talbot interferometry giving values from \sim 1.34 at the surface to 1.44 in guinea pig nucleus and 1.54 in the mouse nucleus.²⁰ Differences in RI are also reflected in differences in protein concentration, which for many fish lenses can exceed 1 g/mL, whereas human lenses have a concentration of only 0.32 g/mL.^{3,21}

However, γ -crystallins also have other requirements. Like other crystallins, they must be highly stable, existing without turnover for the life of the organism, and they must be able to maintain the short-range order of the high protein concentration lens cytoplasm necessary for transparency.²² This would be particularly demanding in the extremely dense fish lens. Even at a concentration of 500 mg/

mL, the average distance between spherical proteins is only approximately half their radius, and at 750 mg/mL on average only two water layers can be accommodated between proteins. For some γ -crystallins, the balance of interactions required for short-range order is delicate and they can undergo reversible, temperature-dependent phase separation below physiological conditions.^{3,23,24}

The functional roles of γ -crystallins in the lens are still not fully understood. It has been proposed that the ability of the paired tryptophans to quench UV has a direct role in protection of the retina.⁷ Recently, it has been shown that mouse γ S-crystallin has a chaperone-like role in stabilizing F-actin in the lens, suggesting that γ -crystallins may participate in maintenance of the supramolecular organization of the lens cytoplasm.²⁵ In the current work, we compared stability, aggregation, and solution properties of zebrafish γ M2b and γ M7-crystallins with mouse γ S and human γ D-crystallins, two well-studied examples of mammalian γ -crystallins^{6,7,26–28} to determine what properties have been conserved or modified during the evolutionary divergence of these rather different members of the γ -crystallin family.

Results

Recombinant proteins

Two examples of zebrafish γ M, γ M2b, and γ M7 were selected to represent high methionine content and different numbers of tryptophans while avoiding longer N-terminal extensions.¹³ For comparison, human γ D, the major γ -crystallin of the human lens nucleus, and mouse γ S, which is expressed at higher levels in the less-dense lens cortex, were also selected. None of these proteins under phase separation. Figure 1 shows the aligned mature protein sequences with residues of interest highlighted.

All four recombinant proteins were expressed in bacterial hosts and were abundant in the soluble fraction. The proteins were purified by ion-exchange and size-exclusion chromatography, with the final purity above 95% [Fig. 2(A)]. γ M7, γ S, and γ D were all stable at concentrations of at least 20–40 mg/mL for weeks at 4°C in working buffer. In contrast, γ M2b was stable in solution at 10 mg/mL but at 15 mg/mL precipitated out of solution overnight [Fig. 2(B)]. All four proteins exhibited similar far UV CD spectra typical of the γ -crystallin family, corresponding to a predominantly β -sheet secondary structure with a characteristic minimum at 218 nm and a shoulder at 235 nm [Fig. 3(A)]. Trp fluorescence emission spectra were assessed by excitation at 295 nm and emission from 310 to 420 nm [Fig. 3(B)]. The proteins had similar spectra, although γ M2b, with only one Trp, had higher fluorescence emission than other proteins, consistent with the

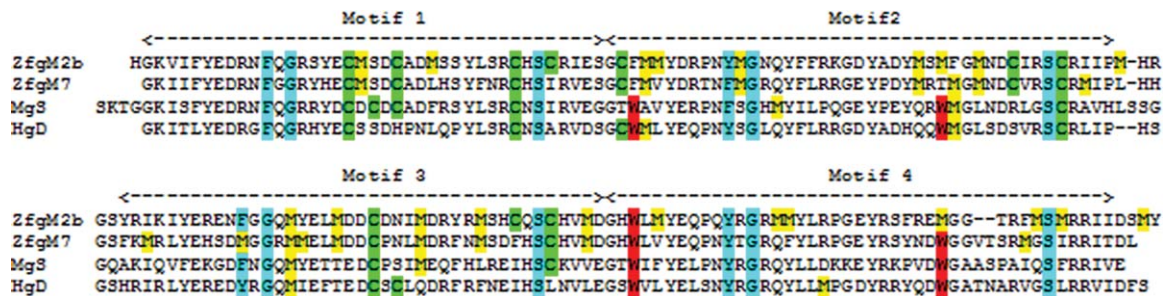


Figure 1. Protein sequence alignment of γ -crystallins. Sequences for γ M2b and γ M7 or zebrafish were aligned with those of mouse γ S and human γ D using CLUSTAL W. The positions of the four structural motifs (1–4) are indicated. Key residues of the β - γ -crystallin motif template are highlighted in blue. Other highlights show positions of methionine (green), cysteine (yellow), and tryptophan (red).

UV-quenching of paired Trp residues.⁷ The slight red shift to 328 nm for mouse γ S suggests a relatively higher solvent exposure for the core Trp residues in this protein. Similar results for γ S and γ D have been reported in other studies.^{6,7} Overall, the results show that all proteins have well-ordered secondary and tertiary structure.

Thermal stability

For lens transparency, crystallins must avoid formation of light scattering aggregates. The propensity for aggregation was examined by thermal stability for 0.5 mg/mL solutions of proteins in working buffer measured by solution turbidity at 600 nm [Fig. 4(A)]. The four γ -crystallins exhibited a wide range of behaviors under these conditions. γ M2b and γ M7 had lower transition temperatures than the mammalian proteins with turbidity increase beginning at about 42°C. Mouse γ S began to scatter above 47°C, whereas human γ D showed no turbidity up to 63°C. The comparative ranking of these results is consistent with previous measurements that compared loss of secondary structure with increasing temperature by monitoring loss of CD signal at 218 nm.²⁹ Although trends were similar for turbidity and CD measurements for each protein, aggregation consis-

tently began at a lower temperature than measurable loss of β -sheet structure.

Two versions of the chaperone-like protein human α B-crystallin, a small heat-shock protein,^{30,31} were also tested in the same assay. The full-length, multimeric protein (α B-F) aggregated around 60°C [Fig. 4(A)]. In contrast, α B-D, a truncated, dimeric form, previously used for structure determinations,³⁰ was remarkably resistant to formation of light scattering aggregates in this assay up to 80°C.

It is thought that α -crystallins have an important role in capturing unfolded elements of lens proteins, thereby inhibiting formation of light-scattering aggregates in the lens.³¹ To test the ability of human α B-crystallin to retard aggregation of the unfolding γ -crystallins, a critical temperature (T_c) was defined for each γ -crystallin, based on the aggregation profiles shown in Figure 4(A). In each case, a range of temperatures was tested in the early linear phase of increasing turbidity. Both γ M-crystallins began to show turbidity at 42°C and for both a T_c of 51°C was used for chaperone studies. For γ S, which exhibited a narrower range of temperatures up to maximum turbidity, both 52 and 56°C were tested. For the highly stable γ D, T_c was 72°C.

Proteins were held at T_c and solution turbidity was measured at 600 nm every 10 min (Fig. 5).

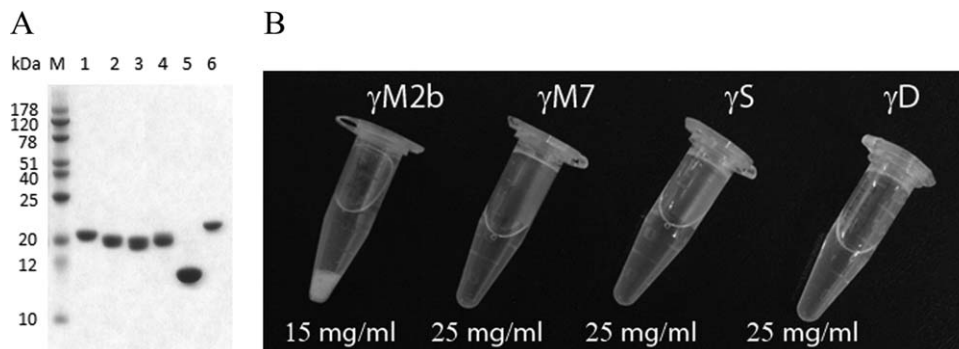


Figure 2. Expression of recombinant crystallins. A: 12% Bis-Tris SDS PAGE of chromatography-purified proteins showed purity above 95%. Lane 1: mouse γ S-crystallin, Lane 2: zebrafish γ M2b, Lane 3: zebrafish γ M7, Lane 4: human γ D, Lane 5: human α B dimer form, Lane 6: human α B full length. B: Solubility of purified recombinant proteins. γ M2b was not stable in solution above 10 mg/mL concentration and precipitated overnight at 4°C at 15 mg/mL.

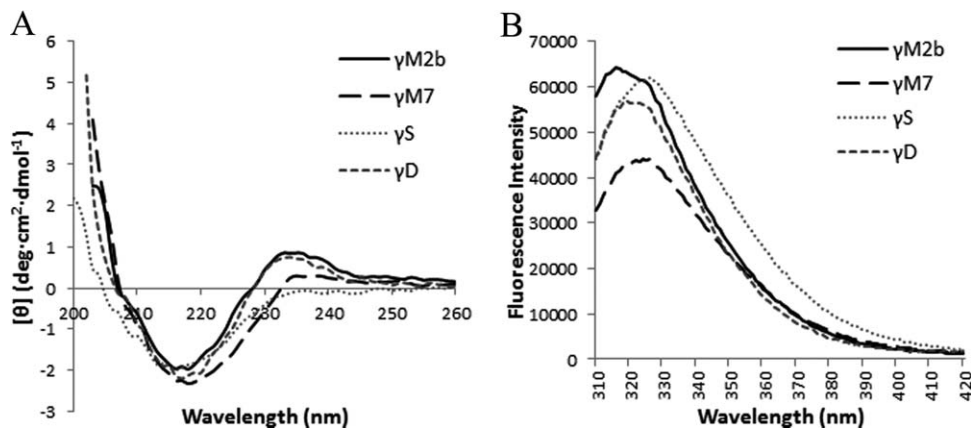


Figure 3. Secondary and tertiary structure of diverse γ -crystallins in solution. Far-UV CD spectra of zebrafish γ M2b, γ M7, mouse γ S, and human γ D at a concentration of 0.5 mg/mL in working buffer at 20°C. All four displayed the negative ellipticity at 218 nm indicative of β -sheet secondary structure and common to γ -crystallins. Fluorescence emission spectra of γ M2b, γ M7, γ S, and γ D. Solutions were excited at 295 nm, and emission spectra were collected from 0.20.

Without addition of α B, turbidity for each protein increased until precipitation occurred. However, there was a marked difference between the behavior of the two γ M-crystallins and the mammalian γ S and γ D proteins, with paired tryptophans in each domain, under these conditions. Both the γ Ms showed a sharp, linear increase in turbidity with no significant lag time and achieved maximum OD600 of 1-1.2 over the course of the experiment. In contrast, both mammalian proteins had a much slower increase in turbidity than the fish proteins. Mouse γ S showed similar profiles at both 52 and 56°C.

Addition of human α B reduced the development of heat-induced turbidity in a dose-dependent manner for all four γ -crystallins but to varying degrees and with different kinetics. Not only did full-length

α B exhibit the expected chaperone-like behavior, significantly retarding turbidity for all four proteins, but the truncated, dimeric form, α B-D, also showed some ability to retard aggregation, whereas non-HSP control proteins (BSA and Cytochrome C) showed no effect at the same mass ratios (not shown). For both γ M2b and γ M7, addition of full-length α B-F significantly reduced turbidity at γ : α mass ratios of both 1:3 and 1:5. α B-D held turbidity of heat-treated γ M7 to about 30% of maximum for 2 h, consistent with stabilization of smaller, aggregates. For γ M2b, the addition of dimeric α B-D had little effect on the development of turbidity up to 30 mins, but then slowed the rate of increase.

γ S was protected from aggregation by α B in a dose-dependent manner. However, because of the much slower increase in turbidity seen for the mammalian proteins than for the γ Ms, the effects over the time course of the experiment were less marked. For γ S, α B-F again gave the strongest protection, whereas α B-D had a smaller effect. Because the T_c for γ D exceeded that of α B-F, protection could only be examined for α B-D, which gave similar results to those seen for γ S.

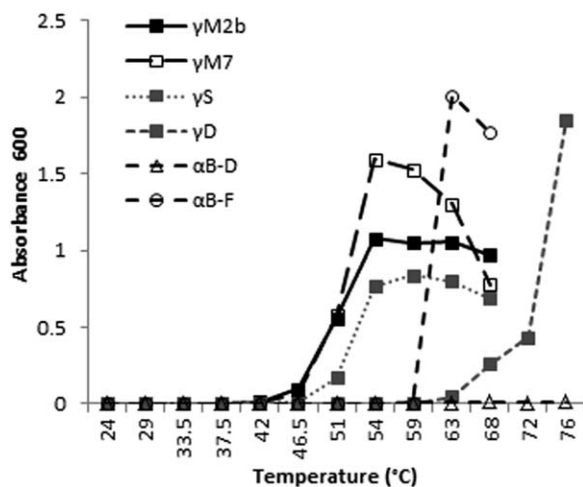


Figure 4. Aggregation behavior of γ -crystallins. Thermal stability of proteins at a concentration of 0.5 mg/mL in working buffer at increasing temperatures measured by turbidity (Absorbance 600 nm). The temperature was increased in every 5°C increment. The protein solution was equilibrated at each temperature for 10 min.

Chemical denaturation

Proteins were exposed to increasing concentrations of GdnHCl and the loss of organized secondary structure was estimated by CD spectroscopy, based on the magnitude of the signal at 218 nm as a measure of β -sheet content. Unfolding of mammalian γ -crystallins has usually been monitored by Trp fluorescence, but this option is not suitable for the fish proteins. For all four proteins, with increasing concentration of denaturant, the magnitude of the characteristic 218 nm minimum decreased until the spectrum switched to a profile consistent with random coil conformation. However, we noticed that for both γ M7 and γ S, intermediate concentrations of

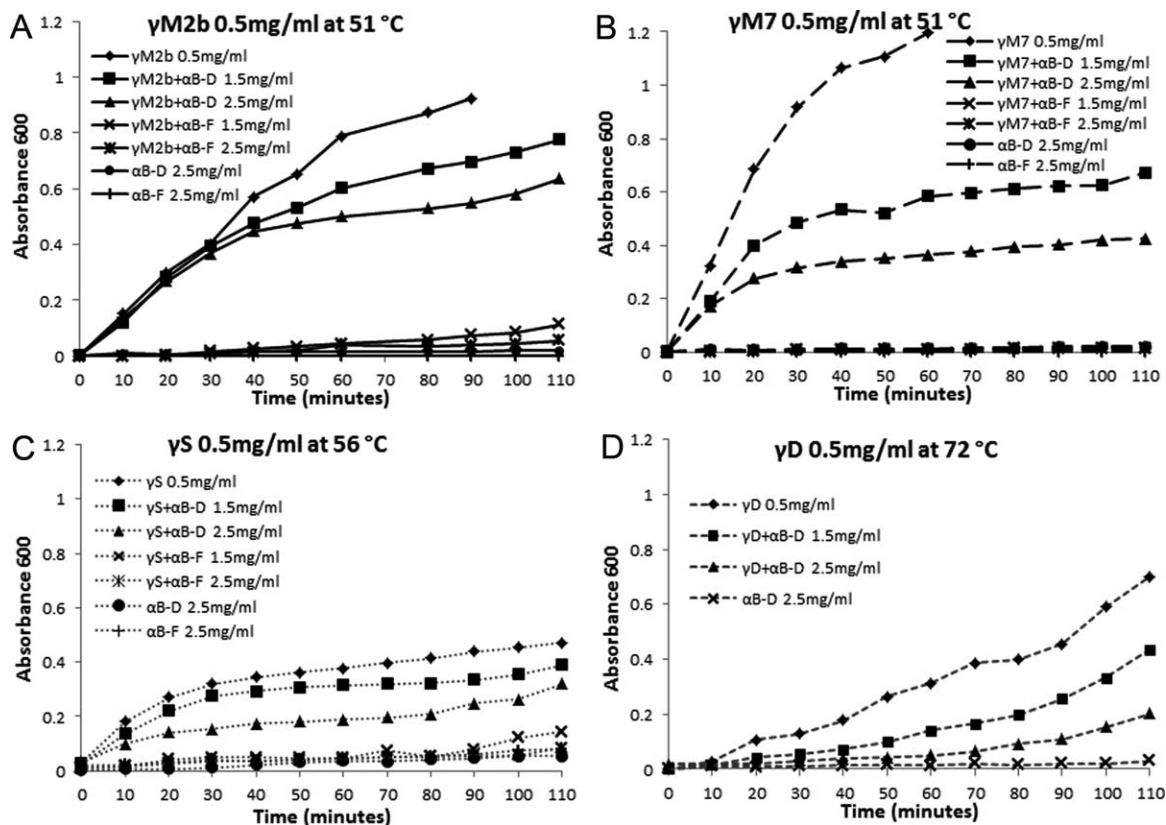


Figure 5. Interaction of heat treated γ -crystallins with human α B-crystallin. Proteins (0.5 mg/mL) were held at temperatures (T_c) that caused increasing turbidity and absorbance at 600 nm was measured over time. Full length (aB-F) or dimeric (aB-D) human α B-crystallin at different mass ratios was added. (A) Zebrafish γ M2b; (B) zebrafish γ M 7; (C) mouse γ S; (D) human γ D. Addition of non-sHSP control proteins had no protective effect (not shown).

GdnHCl caused solution turbidity, presumably due to formation of aggregates. Figure 6 shows the results for zebrafish γ M2b and human γ D, which maintained clear solutions over the range of denaturant concentration.

In contrast to the thermal unfolding results,²⁹ γ M2b exhibited a biphasic pattern of loss of β -sheet under chemical denaturation [Fig. 6(A)] with an apparently stable folding intermediate at 0.8–1.6 M . The midpoint of the first folding transition to the intermediate was about 0.5 M , whereas the second rapid transition to complete loss of β -sheet signal occurred with a midpoint of about 1.9 M . γ D was much more resistant to unfolding with little structure change below 2.2 M GdnHCl and a sharp loss of ellipticity by 3.6 M [Fig. 6(D)].

Crystallin density and hydrodynamic shape in solution

Protein density and shape asymmetry are key parameters governing solution behavior at the extremely high concentrations present in vertebrate lenses. We conducted a density contrast SV experiment with three γ -crystallins in solutions with different fractions of $H_2^{18}O$. Because the oxygen isotope provides the solvent density contrast, hydro-

gen bonds remain constant and no H/D exchange occurs as in solutions with D_2O heavy water. The SV runs at 50,000 rpm were performed side-by-side and monitored by absorbance at 280 nm. From the global analysis of all boundary profiles at all data sets,³² an excellent fit was achieved, with root-mean-square error well within the usual noise of the data acquisition (Fig. 7) and simultaneously the partial-specific volume and the sedimentation coefficient distribution $c(s)$ were obtained (Fig. 8). For γ D-crystallin, a standard SV experiment in H_2O based working buffer was performed to determine the sedimentation coefficient distribution (Fig. 8). All proteins exhibited a major peak, but human γ D consistently exhibited a small degree of polydispersity (up to $\sim 10\%$) of unknown origin, which varied among batches. We were not able to reduce this polydispersity sufficiently for further SV analysis.

Table I summarizes the measured protein partial-specific volumes, $v_{(SV)}^-$, along with the compositional predictions, $v_{(aa)}^-$. The comparison of the values for the partial-specific volume theoretically predicted based on the amino acid composition with the average partial-specific volume of 0.735 mL/g predicted for all human proteins (which exhibit a normally distributed spread of values with standard

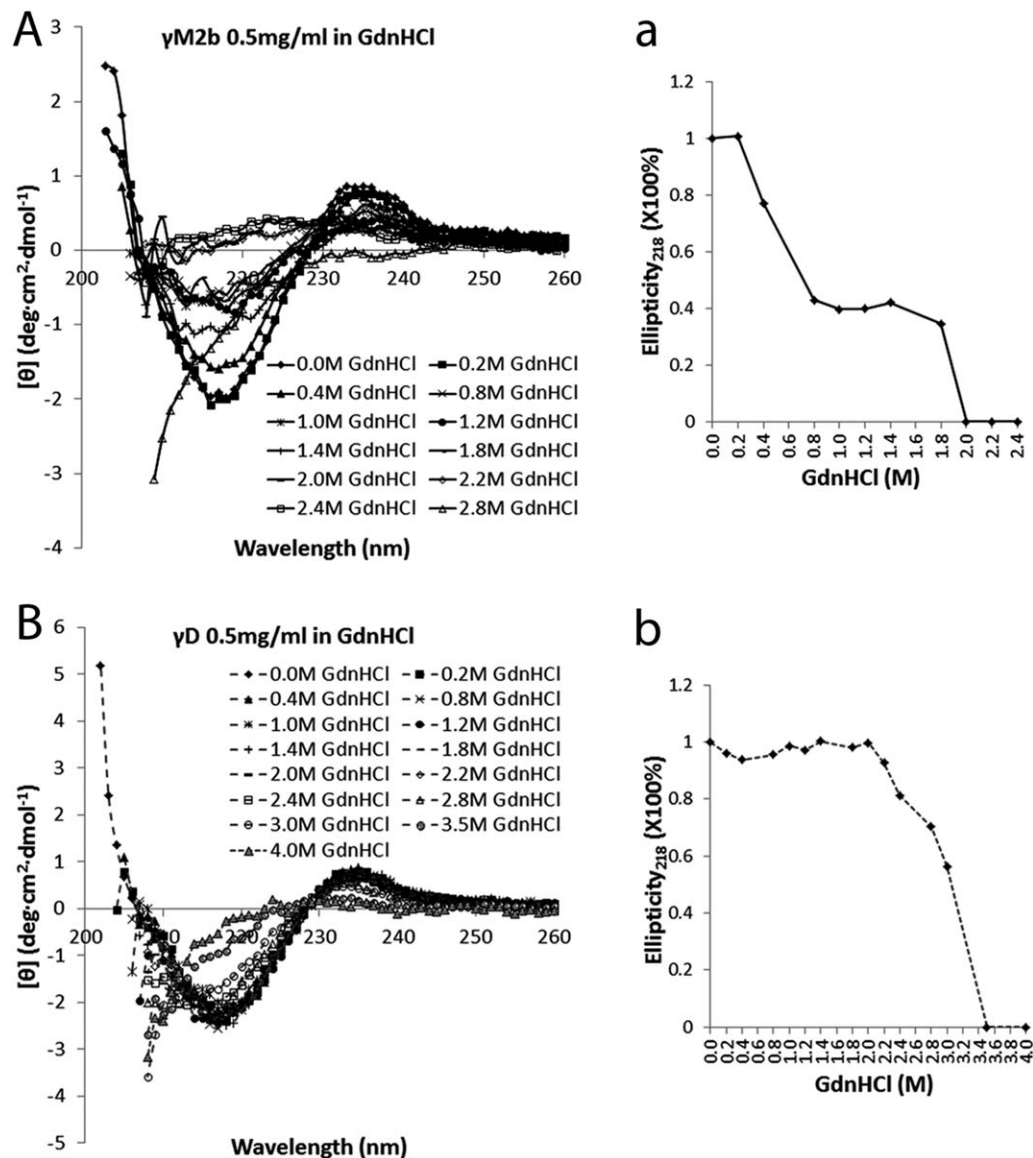


Figure 6. Effects of denaturant on secondary structure in zebrafish and mammalian γ -crystallins. Changes in the secondary structure of zebrafish γ M2b (A) and human γ D (B) were monitored by far-UV CD in a range of concentrations of GdnHCl. The magnitude of ellipticity at 218 nm, estimated by the difference in values at 210 and 218 nm, was used as a measure of β -sheet content and is shown in panels (a) and (b).

deviation of 0.010 mL/g)¹⁶ shows that all lens γ -crystallins have an unusually high abundance of amino acids with higher density, which would be expected to produce a more compact particle. Furthermore, all γ -crystallins are unusually rich in amino acids with polarizable electrons that produce high refractive index increments. Experimental partial-specific volumes can capture, in addition to the amino acid composition, effects such as preferential solvation and charge. The experimentally measured partial-specific volume in phosphate buffer saline for γ M7 from H₂O/H₂¹⁸O density contrast SV was 0.723 (0.713–0.735) mL/g, slightly higher than the amino-acid composition-based theoretical prediction, but consistent with the independently determined value of 0.721 mL/g from sucrose density

contrast sedimentation equilibrium (SE) experiments.⁵¹ Similar is true for γ M2b, which yielded a value of 0.718 mL/g by SV, consistent with the value of 0.716 mL/g by SE. The smallest values were obtained for γ S, with 0.717 mL/g by SV and 0.703 mL/g by SE. These values are distinctly below the average for the human proteome.

In addition to the high density, all γ -crystallins also share a high level of structural compactness of folding. The hydrodynamic translational frictional ratio, f/f_0 , measures the ratio of the Stokes radius to the radius of a perfect smooth solid sphere of equal mass and density. From the measured sedimentation coefficient and partial-specific volume and the known molecular weight, we determined frictional ratios of 1.21 for both γ S and γ D and comparable

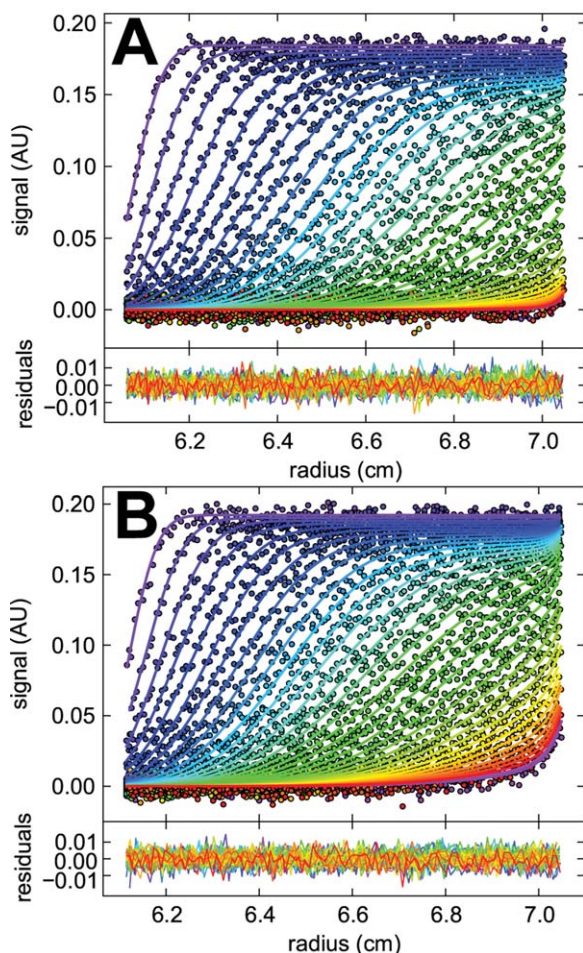


Figure 7. Density contrast velocity sedimentation probing crystallin hydrodynamic shape and partial-specific volume. SV concentration profiles of mouse γ S conducted in 0% (A) and 80% (B) H_2^{18}O monitored by absorbance at 280 nm at 50,000 rpm. Experimental data are depicted as circles (for clarity showing only every 2nd point and 2nd scan) and the best-fit profiles from the global $c(s)$ sedimentation coefficient distribution model to data from all solvent densities are depicted as solid lines, with the residuals expanded below. For each trace, the color temperature corresponds to time after start of sedimentation.

values of 1.17 and 1.21 for γ M7 and γ M2b (with errors of $\sim \pm 0.07$ arising from the propagation of errors in the partial-specific volume and uncertainties of the s -values). These values are at the lower end of the 1.2–1.5 range of values for typical hydrated proteins ranging in shape from rather globular to elongated^{33,34} and are only slightly above the value of 1.12 for a perfect compact smooth protein sphere with standard 0.3 g/g hydration.

Discussion

Because lens fiber cells are terminally differentiated, enucleated cells,³⁵ crystallins must exist without turnover for long periods of time. Individual proteins need to have stable folded structures resistant to

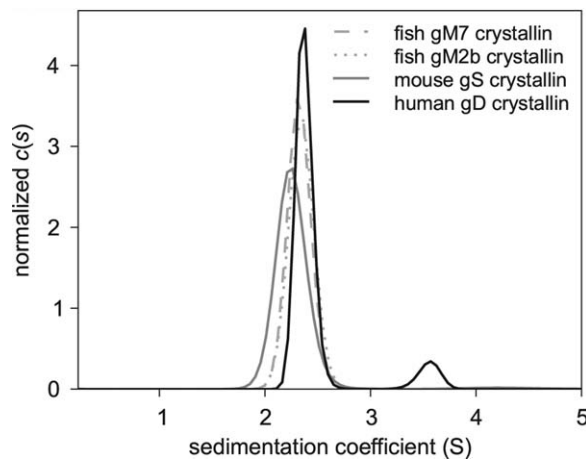


Figure 8. Sedimentation coefficient distributions. Sedimentation coefficient distributions $c(s)$ derived from the global analysis of density contrast sedimentation velocity experiments for mouse γ S, zebrafish γ M2b, and γ M7, or from standard $c(s)$ analysis for human γ D, respectively.

aggregation. The γ -crystallins (and the related β -crystallins) have highly symmetrical structures with each of two domains consisting of characteristic, tightly packed β -sheet sandwiches built from modified Greek key motifs.^{3,36} Several residues key to the folding pattern are highly conserved. However, the basic template of the fold is robust and highly divergent domains in proteins of the $\beta\gamma$ -crystallin superfamily are still able to adopt the core β -sheet structure.³⁷

γ -crystallins seem to have been evolved in the earliest vertebrate lenses,^{38,39} and they are particularly abundant and diverse in the lenses of modern fish.¹³ Under water, the cornea makes little contribution to light refraction so that all of the focusing power for image formation comes from the lens. Consequently, fish lenses tend to be quite spherical and “hard” with high protein concentration and high refractive index. Although the refractive index of the human lens has been measured using OCT giving a peak value of 1.42 for the nucleus,¹⁸ similar measurements for zebrafish lens gave a peak value of 1.54.¹⁹

Although α - and β -crystallins and γ S- and γ N-crystallins have orthologs in fish and mammals,¹³ the large class of γ M-crystallins is present in fish but not in terrestrial vertebrates. It seems likely that these proteins have evolved specifically to contribute to the properties of the fish lens.

One of the most notable features of the γ M-crystallins is their unusually high contents of methionine and the other sulfur-containing residue, cysteine. These residues are also relatively abundant in mammalian γ -crystallins, although not as markedly as in fish. Methionine and cysteine have been thought of as liabilities for long-lived lens proteins; their sulfur atoms are potential targets for

oxidation, creating charged forms or intra- or intermolecular bonding that might lead to formation of light-scattering aggregates. Indeed, oxidation of methionine and cysteine has long been of interest in cataract research.^{9–11} However, it has recently been pointed out that all the major crystallins have relatively high contents of amino acids with higher than average refractive index increments (generally the larger side chains), including methionine, and that this is likely an adaptation that contributes to the refractive power of the lens.^{15,16} It would appear to have been taken to an extreme in the γ M-crystallins of the fish lens.

In addition to the thermodynamic stability of individual proteins, crystallins must maintain the short range order of the lens cell cytoplasm on which transparency depends.^{22,35} They need to be resistant to phase separation (creating protein-rich domains in solution)²⁴ formation of light-scattering aggregates or even crystallization under the conditions of high macromolecular crowding that exist in the lens.¹⁷ Indeed, the polydispersity conferred by the multiplicity of γ M-crystallins might contribute to the maintenance of short range order in the high density of the fish lens.

γ -crystallins are thus subject to several strong constraints and it is likely that there are evolutionary trade-offs as proteins adapt to the needs of different species. For example, the high content of methionine in γ M-crystallins may have advantages for refractive power or some other property but could compromise other functions. To explore what is conserved and what can vary, we have compared the stability of secondary structure, the resistance to aggregation, the interaction with a lens chaperone-like proteins, α B-crystallin,³¹ and the hydrodynamic and hydration properties of two proteins of the dense fish lens, γ M2b and γ M7 from zebrafish, with two mammalian proteins, human γ D, the major γ -crystallin of the human lens nucleus, and mouse γ S, the major γ -crystallin of the mammalian lens cortex.

All four proteins conserve the basic repeat structure of the Greek key motifs and the key residues of the folded β -hairpin supersecondary structure that defines the family, including the Tyr-corners. However, although γ D and γ S also conserve the paired tryptophan residues in the core of each domain, γ M7 has only one pair in the C-terminal domain, whereas γ M2b has a single unpaired tryptophan. It has been shown that the paired Trps are involved in a mechanism of UV quenching that could have a protective role for the eye.⁷ This could be of value for terrestrial species exposed to UVB, but would be of less value to aquatic species. Even so, other members of the β - γ -crystallins in zebrafish, β -crystallins, γ S-crystallins, and γ N-crystallins, do contain the conserved Trp-pairs,¹³ suggesting that their original role was

not related to UV quenching but to some other function, perhaps in stabilization of the domain fold.

CD-spectra for all four proteins are similar, consistent with the well-folded β -sheet structure known for the mammalian proteins.^{40,41} Trp fluorescence spectra for the γ M7, γ D, and γ S (with paired Trps) are similar but γ M2b, with only a single Trp has higher fluorescence, showing again that pairing is required for UV quenching.⁷

All four recombinant proteins were found in the soluble fraction however, γ M2b was notably less soluble than typical γ -crystallins and saturated at only 15 mg/mL. This is reminiscent of some cataract-causing mutants, such as the P23T mutant of human γ D, with reduced solubility.⁴⁰ It suggests that in the lens, interaction with other components is required to keep γ M2b in solution.

Differences in stability of the proteins were apparent even at low concentration (0.5 mg/mL). Both in terms of heat-induced aggregation and loss of secondary structure by heat or chemical denaturation, γ M2b and γ M7 had lower stability than γ D and γ S. Because body temperature of the zebrafish is lower, it is not surprising that requirements for thermal stability of lens proteins would also be lower; however, there is certainly no evidence that high methionine content contributes to thermal stability. A more likely cause of reduced stability is the “replacement” of tryptophans in the cores of the fish proteins. Indeed, the NMR structure analysis of γ M7 shows that the N-domain, lacking core tryptophans, is less tightly packed than the C-domain.²⁹ The most stable protein of the four was human γ D. This protein is largely synthesized in the embryonic lens, which constitutes the core or nucleus of the lens, and therefore, may survive without turnover for a century in humans. This may explain its requirement for higher thermodynamic stability.

However, an important contributor to stability in the lens is the extremely high intracellular protein concentrations. Intracellular crowding will provide additional forces stabilizing the most compact state.^{42,43} The significantly more crowded conditions in fish lenses leaves little space for unfolding and may thereby provide stabilizing contributions for the γ M proteins with lower overall structural stability.

The different proteins also show differences in their profiles of unfolding. Previous measurement of thermal denaturation gave essentially monophasic unfolding curves for all four proteins, suggesting that there is no partially stable intermediate under these conditions.²⁹ However, chemical denaturation, monitored by loss of the 218 nm minimum in CD, suggested that zebra fish γ M2b underwent biphasic loss of secondary structure with a partially stable intermediate form. This most likely reflected a difference in stability of the two domains, with lower

Table I. Properties of Diverse Gamma-Crystallins

Crystallin	MW (kDa)	Methionine (%)	dn/dc ₍₅₈₀₎ (mL/g)	V ⁻ _(aa) (mL/g)	v ⁻ _(SV) (mL/g)	v ⁻ _(SE) (mL/g) ^a	B ₁ (g/g) ^a	f/f ₀ (hyd) ^a	f/f ₀ (exp)
γS	20,719	2.3	0.199	0.717	0.717	0.703	0.22	1.30	1.21
γD	20,607	2.3	0.200	0.712	n.d.	n.d.	n.d.	1.21	1.21
γM7	20,776	9.8	0.203	0.708	0.723	0.721	0.12	1.24	1.17
γM2b	21,917	13.3	0.203	0.702	0.718	0.716	0.15	n.d.	1.21

All values refer to standard conditions at 20°C.

^a Values for the partial-specific volume measured in sedimentation equilibrium sucrose density contrast experiments (v⁻_(SE)), the preferential water binding coefficient (B₁), and the theoretical solution structure-based frictional coefficient assuming standard hydration (f/f₀ hyd.) are taken from Ref. 51.

stability for the N-terminal domain, which lack the usually conserved tryptophans.

The proteins also differ in their interaction with αB-crystallin under thermal stress. The full-length human αB gave substantial protection of γM2b, γM7, and γS, although it was not itself stable under the conditions needed to stress γD. Interestingly, the truncated dimer form of αB also had some ability to modify aggregate formation. The dimer retarded aggregation for both mammalian proteins and γM2b and γM7 although with noticeable differences in the profile of increasing turbidity. This could reflect differences in affinity for dimer binding to unfolding intermediates of the two fish proteins.

Finally, the hydrodynamic properties of the proteins were compared by AUC. Here, the striking result was that fish and mammal γ-crystallins, despite considerable differences in composition, aggregation behavior and unfolding showed close similarities in solution behavior. Both in terms of mass density (and the related refractive index increment), the proteins are far from the mean expected for all proteins, with properties consistent with the demands of highly concentrated intracellular environments (Table I). They have unusually low frictional ratios, suggesting that they have low hydration and a low propensity for sticky interactions with solvent and, perhaps, with other proteins. These properties are likely due to the conserved tertiary fold of the proteins and the way in which surface side chains pack close to the molecular surface, often as part of a network of polar interactions.

γ-Crystallins are not alone in the lens. They exist alongside the larger and rather polydisperse, multimeric α- and β-crystallins and cytoskeletal and membrane bound proteins of several kinds. These complex mixtures need to maintain short range order and to avoid formation of light-scattering centers, either through unfolding, aggregation or phase separation. A major role of the γ-crystallins may be to act as a “molecular lubricant” smoothly separating and spacing the other components of the lens. Although other features of γ-crystallins that contribute to refractive index, UV protections or thermodynamic stability may be subject to compromise through evolutionary modification and specializa-

tion, the basic role as a highly compact stabilizer of the lens cytoplasm seems to be highly selected during evolution.

Materials and Methods

Sequence alignment

GenBank accession numbers are as follows: *Danio rerio* γM2b (BC163189.1) and γM 7 (BC162654.1); mouse γS (NM_009967.2) and human γD (NM_005267.4). Alignment was performed using CLUSTAL W in BioEdit.⁴⁴

Protein expression and purification

Full length ORF clones for zebrafish γM2b and γM7 and for human γD were selected from the NEIBank resource.^{45–47} Inserts were amplified by PCR using primers with added restriction sites (*italics*):

GM2BNDE: 5' ACATATGCATGGAAAGGTCATC TTCTAC 3';

GM2BXHO: 5' TCTCGAGTTAGTACATAGAGT CTATGATAC 3';

GM7NDE: 5' ACATATGGGAAAGATTATCTTTT ATGAAG 3';

GM7XHO: 5' CCTCGAGTTAGAGATCCGTGATT CGTC 3';

HGDNDE: 5' CATATGGGGAAGATCACCCCTCT AC 3';

HGDHXHO: 5' CTCGAGTCAGGAGAAATCTATG ACT 3';

and were cloned into NdeI/XhoI sites of pET-17b (Novagen, Madison WI). The mouse γS expression clone has been described previously.²⁶ Proteins were expressed in *Escherichia coli* BL21(DE3)pLysS. Colonies were grown in LB broth with ampicillin (50 mg/mL) and chloramphenicol (34 mg/mL in ethanol). Protein production was induced by 1 mM IPTG with culturing at 20°C overnight. Bacteria were pelleted by centrifuging at 4°C for 15 min and resuspended in 50 mM Tris-HCl 7.2, 10 mM EDTA, 300 mM NaCl. Pellets were lysed by repeated sonication with 2 sec burst and 5 sec break for 10 min working time. Cell lysate supernatant was dialyzed to working buffer (50 mM Tris, pH 8.5, 1 mM dithiothreitol, and 1 mM EDTA). Dialyzed protein was loaded on a Mono Q 5/50 GL anionic exchange column (Amersham Pharmacia Biotech)

using the AKTA Explorer 100 (Amersham Pharmacia Biotech) purification system. Fractions were monitored by UV absorbance and collected in a range of 20–30% NaCl. Combined fractions were loaded onto a HiLoad 16/60 Superdex 75 size exclusion column (Amersham Pharmacia Biotech) equilibrated by the working buffer. Fractions were analyzed by SDS PAGE using NuPage® 12% Bis-Tris polyacrylamide gels (Novex, San Diego). Proteins of interest were pooled and concentrated by Amicon Ultra centrifugal device with 3 kDa cutoff (Millipore, Billerica MA).

Full-length human α B-crystallin ORF was similarly cloned using PCR primers: HABNDE1: 5' CTAGCCCA-TATGGACATCGCCATCCACCACCCTG 3'; HABXHO 1: 5' AAGAAACTCGAGCTATTTCTTGGGGGCTGCGG TGA 3'. The expression vector for the truncated dimer of human α B-crystallin was described previously.³⁰

Spectroscopy

Circular dichroism (CD) spectra were recorded on a Jasco J-810 spectropolarimeter (Jasco International Co., Hachioji, Tokyo, Japan) at 20°C. Far UV CD experiments were performed at protein concentration of 0.5 mg/mL in working buffer (50 mM Tris, pH 8.5, 1 mM dithiothreitol, and 1 mM EDTA) containing 0–4 M GdnHCl using a 1-mm path length cuvette. Data were collected over the wavelength range of 320–190 nm at 0.2-nm intervals. Three scans were averaged and normalized by subtracting the base line recorded for the buffer or the buffer having the same GdnHCl concentration. The results were plotted as ellipticity (mdeg) versus wavelength (nm).

Fluorescence emission spectra were taken on a PTI fluorometer (Photon Technology International, Trenton, NJ) at 20°C.

Thermal and chemical denaturation

A total of 0.5 mg/mL protein in buffer was placed in an airtight, 1 cm path length, quartz cuvette. Samples were incubated in a heating block at each temperature point for 10 min before the measurements. The actual temperature at each time point was measured by thermocouple probe. Thermal denaturation was monitored at absorbance OD 600 in 5°C intervals over the temperature range of 25–90°C.

Chemical unfolding was performed by incubating the protein with 0–7 M guanidinium hydrochloride (GdnHCl) at 37°C for 2 h followed by 4°C overnight. Protein unfolding was monitored at 20°C by CD spectroscopy. Loss of organized β -sheet was monitored by calculating the magnitude of the difference in ellipticity at 218 and 210 nm as a measure of the 218 nm minimum.

Temperature-dependent α B chaperone assay

γ -crystallins at 0.5 mg/mL were incubated with 3-fold or 5-fold mass amounts of full-length or trun-

cated dimer human α B-crystallin in an airtight, 1 cm path length, quartz cuvette at the chosen temperature (T_c). The ability of α B to prevent the aggregation of substrate proteins was monitored by absorbance at OD 600. All experiments were performed in triplicate. Similar experiments were also performed using the same mass amounts of BSA or cytochrome C (Sigma-Aldrich, St. Louis, MO) as non-heat shock protein controls for the effects of α B.

Sedimentation velocity analytical ultracentrifugation (SV)

SV experiments were performed using analytical ultracentrifuges (ProteomeLab XL-A or XL-I; Beckman Coulter) according to the protocols outlined in Brown et al.³² In brief, chromatographically purified protein samples were prepared in 50 mM Tris-HCl 8.5, 1 mM EDTA, and 1 mM DTT, pH 8.50 and diluted into H₂O, or isotopically enriched H₂¹⁸O to achieve H₂¹⁸O/H₂O ratios of 0, 50, and 80% (v/v). For density contrast SV of mouse γ S, the final protein concentration was 0.42 mg/mL. One hundred microliter of SV samples was loaded into 3-mm double sector centerpieces, temperature equilibrated to 20°C, and sedimentation at 50,000 rpm was monitored using absorbance optics at 280 nm. The sedimentation velocity profiles for proteins in solutions of increasing density were fit globally to obtain a diffusion-deconvoluted sedimentation coefficient distribution $c(s)$ along with an estimate of the partial-specific volume using SEDPHAT.³² Error estimates were derived from the application of the error surface projection method and F-statistics to the global analysis, and amounted to $\sim \pm 0.01$ mL/g. SV experiments of the human γ D-crystallin in the working buffer were performed with 0.13 mg/mL of protein loaded into 12-mm centerpieces. Corrections for the recorded scan time corrections were applied as described in Ref. 48. All plots of analytical ultracentrifugation concentration profiles and their fits were made with the software GUSI (<http://biophysics.sw-med.edu/MBR/software.html>, kindly provided by Dr. Chad Brautigam).

Compositional predictions of the partial-specific volume were based on the tabulated amino acid partial-specific volumes by Cohn and Edsall,⁴⁹ and compositional predictions of the refractive increment were based on the tabulated data by McMeekin and coworkers,^{16,50} both as implemented in SEDFIT.

References

1. Wistow G (1993) Lens crystallins: gene recruitment and evolutionary dynamism. *Trends Biochem Sci* 18: 301–306.
2. Wistow GJ, Piatigorsky J (1988) Lens crystallins: the evolution and expression of proteins for a highly specialized tissue. *Annu Rev Biochem* 57:479–504.

3. Bloemendal H, De Jong W, Jaenicke R, Lubsen NH, Slingsby C, Tardieu A (2004) Ageing and vision: structure, stability and function of lens crystallins. *Prog Biophys Mol Biol* 86:407–485.
4. Slingsby C, Clout NJ (1999) Structure of the crystallins. *Eye* 13:395–402.
5. Hemmingsen JM, Gernert KM, Richardson JS, Richardson DC (1994) The tyrosine corner: a feature of most Greek key α -barrel proteins. *Protein Sci* 3:1927–1937.
6. Kosinski-Collins MS, Flaugh SL, King J (2004) Probing folding and fluorescence quenching in human gammaD crystallin Greek key domains using triple tryptophan mutant proteins. *Protein Sci* 13:2223–2235.
7. Chen J, Callis PR, King J (2009) Mechanism of the efficient quenching of tryptophan fluorescence in human gamma D- and gamma S-crystallins: the gamma-crystallin fold may have evolved to protect tryptophan residues from ultraviolet photodamage. *Biochemistry* 48:3708–3716.
8. Wistow G, Turnell B, Summers L, Slingsby C, Moss D, Miller L, Lindley P, Blundell T (1983) X-ray analysis of the eye lens protein gamma-II crystallin at 1.9 Å resolution. *J Mol Biol* 170:175–202.
9. Harding JJ, Dille KJ (1976) Structural proteins of the mammalian lens: a review with emphasis on changes in development, aging and cataract. *Exp Eye Res* 22:1–73.
10. Truscott RJ (2005) Age-related nuclear cataract-oxidation is the key. *Exp Eye Res* 80:709–725.
11. Moreau KL, King JA (2012) Protein misfolding and aggregation in cataract disease and prospects for prevention. *Trends Mol Med* 18:273–282.
12. Chang T, Jiang YJ, Chiou SH, Chang WC (1988) Carp gamma-crystallins with high methionine content: cloning and sequencing of the complementary DNA. *Biochim Biophys Acta* 951:226–229.
13. Wistow G, Wyatt K, David L, Gao C, Bateman O, Bernstein S, Tomarev S, Segovia L, Slingsby C, Vihtelic T (2005) Gamman-crystallin and the evolution of the betagamma-crystallin superfamily in vertebrates. *FEBS J* 272:2276–2291.
14. Greiling TM, Houck SA, Clark JI (2009) The zebrafish lens proteome during development and aging. *Mol Vis* 15:2313–2325.
15. Zhao H, Brown PH, Magone MT, Schuck P (2011) The molecular refractive function of lens gamma-crystallins. *J Mol Biol* 411:680–699.
16. Zhao H, Brown PH, Schuck P (2011) On the distribution of protein refractive index increments. *Biophys J* 100:2309–2317.
17. Zhao H, Magone MT, Schuck P (2011) The role of macromolecular crowding in the evolution of lens crystallins with high molecular refractive index. *Phys Biol* 8:046004.
18. Uhlhorn SR, Borja D, Manns F, Parel JM (2008) Refractive index measurement of the isolated crystalline lens using optical coherence tomography. *Vision Res* 48:2732–2738.
19. Rao KD, Verma Y, Patel HS, Gupta PK (2006) Non-invasive ophthalmic imaging of adult zebrafish eye using optical coherence tomography. *Curr Sci* 90:1506–1510.
20. Hoshino M, Uesugi K, Yagi N, Mohri S, Regini J, Pierscionek B (2011) Optical properties of in situ eye lenses measured with X-ray Talbot interferometry: a novel measure of growth processes. *PLoS One* 6:e25140.
21. Kroger RH, Campbell MC, Munger R, Fernald RD (1994) Refractive index distribution and spherical aberration in the crystalline lens of the African cichlid fish *Haplochromis burtoni*. *Vision Res* 34:1815–1822.
22. Delaye M, Tardieu A (1983) Short-range order of crystallin proteins accounts for eye lens transparency. *Nature* 302:415–417.
23. Benedek GB, Pande J, Thurston GM, Clark JI (1999) Theoretical and experimental basis for the inhibition of cataract. *Prog Retin Eye Res* 18:391–402.
24. Clark JI, Clark JM (2000) Lens cytoplasmic phase separation. *Int Rev Cytol* 192:171–187.
25. Fan J, Dong L, Mishra S, Chen Y, Fitzgerald P, Wistow G (2012) A role for gammaS-crystallin in the organization of actin and fiber cell maturation in the mouse lens. *FEBS J* 279:2892–2904.
26. Sinha D, Wyatt MK, Sarra R, Jaworski C, Slingsby C, Thaug C, Pannell L, Robison WG, Favor J, Lyon M, Wistow G (2001) A temperature-sensitive mutation of Crygs in the murine Opj cataract. *J Biol Chem* 276:9308–9315.
27. Lee S, Mahler B, Toward J, Jones B, Wyatt K, Dong L, Wistow G, Wu Z (2010) A single destabilizing mutation (F9S) promotes concerted unfolding of an entire globular domain in gammaS-crystallin. *J Mol Biol* 399:320–330.
28. Mahler B, Doddapaneni K, Kleckner I, Yuan C, Wistow G, Wu Z (2011) Characterization of a transient unfolding intermediate in a core mutant of gammaS-crystallin. *J Mol Biol* 405:840–850.
29. Mahler B, Chen Y, Ford J, Thiel C, Wistow G, Wu Z (2013) Structure and dynamics of the fish eye lens protein, gammaM7-crystallin. *Biochemistry* 50:3579–3587.
30. Bagneris C, Bateman OA, Naylor CE, Cronin N, Boelens WC, Keep NH, Slingsby C (2009) Crystal structures of alpha-crystallin domain dimers of alphaB-crystallin and Hsp20. *J Mol Biol* 392:1242–1252.
31. Clark AR, Lubsen NH, Slingsby C (2012) sHSP in the eye lens: crystallin mutations, cataract and proteostasis. *Int J Biochem Cell Biol* 44:1687–1697.
32. Brown PH, Balbo A, Zhao H, Ebel C, Schuck P (2011) Density contrast sedimentation velocity for the determination of protein partial-specific volumes. *PLoS One* 6:e26221.
33. Cantor CR, Schimmel PR (1980) *Biophysical chemistry. II. Techniques for the study of biological structure and function*. New York: W.H. Freeman.
34. Serdyuk IN, Zaccai NR, Zaccai J (2007) *Methods in molecular biophysics: structure, dynamics, function*. Cambridge: Cambridge University Press.
35. Bassnett S, Shi Y, Vrensen GF (2011) Biological glass: structural determinants of eye lens transparency. *Philos Trans Roy Soc B* 366:1250–1264.
36. Wistow G, Slingsby C, Structure and evolution of crystallins. In: Dartt DA, Besharse JC, Dana R, Eds. (2010) *The encyclopedia of the eye*. Elsevier, pp 229–238.
37. Aravind P, Wistow G, Sharma Y, Sankaranarayanan R (2008) Exploring the limits of sequence and structure in a variant betagamma-crystallin domain of the protein absent in Melanoma-1 (AIM1). *J Mol Biol* 381:509–518.
38. Shimeld SM, Purkiss AG, Dirks RP, Bateman OA, Slingsby C, Lubsen NH (2005) Urochordate betagamma-crystallin and the evolutionary origin of the vertebrate eye lens. *Curr Biol* 15:1684–1689.
39. Kappe G, Purkiss AG, van Genesen ST, Slingsby C, Lubsen NH (2010) Explosive expansion of betagamma-crystallin genes in the ancestral vertebrate. *J Mol Evol* 71:219–230.

40. Evans P, Wyatt K, Wistow GJ, Bateman OA, Wallace BA, Slingsby C (2004) The P23T cataract mutation causes loss of solubility of folded gammaD-crystallin. *J Mol Biol* 343:435–444.
41. Wu Z, Delaglio F, Wyatt K, Wistow G, Bax A (2005) Solution structure of (gamma)S-crystallin by molecular fragment replacement NMR. *Protein Sci* 14:3101–3114.
42. Zhou HX (2008) Protein folding in confined and crowded environments. *Arch Biochem Biophys* 469:76–82.
43. Tsao D, Minton AP, Dokholyan NV (2010) A didactic model of macromolecular crowding effects on protein folding. *PLoS One* 5:e11936.
44. Hall TA (1999) BioEdit: a user-friendly biological sequence alignment editor and analysis program for Windows 95/98/NT. *Nucl Acids S* 41:95–98.
45. Wistow G, Bernstein SL, Wyatt MK, Behal A, Touchman JW, Bouffard G, Smith D, Peterson K (2002) Expressed sequence tag analysis of adult human lens for the NEI-Bank Project: over 2000 non-redundant transcripts, novel genes and splice variants. *Mol Vis* 8:171–184.
46. Vihtelic TS, Fadool JM, Gao J, Thornton KA, Hyde DR, Wistow G (2005) Expressed sequence tag analysis of zebrafish eye tissues for NEIBank. *Mol Vis* 11:1083–1100.
47. Wistow G, Peterson K, Gao J, Buchoff P, Jaworski C, Bowes-Rickman C, Ebright JN, Hauser MA, Hoover D (2008) NEIBank: genomics and bioinformatics resources for vision research. *Mol Vis* 14:1327–1337.
48. Zhao H, Ghirlando R, Piszczek G, Curth U, Brautigam CA, Schuck P (2013) Recorded scan times can limit the accuracy of sedimentation coefficients in analytical ultracentrifugation. *Anal Biochem* 437:104–108.
49. Cohn EJ, Edsall JT, Density and apparent specific volume of proteins. In: Cohn EJ, Edsall JT, Eds. (1943) *Proteins, amino acids and peptides*. New Jersey: Van Nostrand-Reinhold, Princeton, pp 370–381.
50. McMeekin TL, Groves ML, Hipp NJ, Refractive indices of amino acids, proteins and related substances. In: Stekol J, Ed. (1964) *Amino acids and serum proteins*. Washington DC: American Chemical Society.
51. Zhao H, Chen Y, Rezabkova L, Wu Z, Wistow G, Schuck P (2013) Solution properties of gamma-crystallins: Hydration of fish and mammal gamma-crystallins. *Prot. Sci* 23:88–99.